

The Search for Missing Resonances: the Neutron Anomaly.

Igal Jaeglé for CB-ELSA/TAPS and A2 Collaborations

Department of Physics, University of Basel, Klingelbergstrasse 82, CH-4056 Basel, Switzerland

Abstract. We report the observation of a narrow structure in the invariant mass spectrum of the η -neutron pairs produced in the reaction $\gamma d \rightarrow \eta n(p)$ which is absent in the η -proton pairs produced in the reaction $\gamma d \rightarrow \eta p(n)$. These results are obtained from a liquid deuterium target, the data sample was collected with the Crystal Barrel and TAPS detectors at the electron accelerator ELSA. This structure is also seen in preliminary analyses of the data samples taken by the Crystal Ball and TAPS detectors at the electron accelerator MAMI with a liquid deuterium target and a liquid helium 3 target ruling out a nuclear effect. We report the measurements of the position and width of this narrow structure in the invariant mass spectrum at $W \approx 1665$ MeV and with a FWHM of $\Gamma = 25$ MeV.

Keywords: photoproduction, η -neutron pairs, narrow structure, ELSA, MAMI, Crystal Ball, Crystal Barrel, TAPS

PACS: 13.60.Le, 14.20.Gk, 14.40.Aq

INTRODUCTION

At low energy, the nucleon can be considered to be a bound system made of three quarks, (uud) quarks for the proton and (udd) quarks for the neutron, and is an excellent laboratory to study QCD in the non-perturbative regime. One of the main question concerning this system and which various QCD-based models fail to answer clearly is: what are the degrees-of-freedom of this system ?

Experimentally, the degrees-of-freedom of the nucleon are studied by exciting the nucleon by an external probe. The excited states of the nucleon were first observed in πN scattering in which their contribution was clearly evident as bumps in the total cross section. These measurements allowed a first classification of the excitation spectrum of the nucleon, providing measurement of the masses, widths, quantum numbers, and branching ratios of many baryon resonances [1]. In spite of the large amount of information collected by these experiments, the number of states that were identified was less than that predicted by the standard quark model [2]. A possible explanation is that such “missing” states may decouple from the πN channel, making them undetectable in experiments with pion beams. Other explanations come from theoretical models that are able to predict a smaller number of states based on a reduced set of degrees-of-freedom [3].

The construction of high intensity and high duty cycle electron and photon facilities such as the Elektronen-Stretcher-Anlage (ELSA) in Bonn [4][5] and the Mainzer Mikrotron (MAMI) in Mainz [6][7], opened new possibilities for the study of baryon resonances using electromagnetic probes. These provide information about the resonance and nucleon wavefunctions through the measurement of the helicity amplitudes, i.e. the electromagnetic couplings between nucleon ground state and initial states. In addition electroproduction also allows us to explore baryon structure for different distance scales by varying the photon virtuality. Nowadays electroexcitation processes are a fundamental tool to pursue these studies. However due to the complexity of the baryon spectrum, the proximity and overlapping nature of the various excited states, the measurement of a single channel is not sufficient to complete this research program. To the contrary a thorough study of resonance properties requires the measurement of cross sections, angular distributions, Dalitz plots, as well as polarization observables for different final states. This program is carried since more than ten years by the CB-ELSA/TAPS and A2 Collaborations. In addition the interpretation of the observables extracted from the data requires sophisticated partial waves analyzes.

Most of the data available and taken with a photon probe comes from meson photoproduction off the proton, for the simple reason that there are no free neutron targets. However, the study of neutron excited states is of some interests, since the only way to access the isospin composition of the nucleon resonances is to measure both proton and neutron excited states. Furthermore some excited states might couple stronger to γn for example due to SU(3) symmetries like the Moorhouse selection rules [8].

The non-existence of free neutron targets is solved by using a light nucleus (deuterium or/and helium). The difficulty with using a light nucleus as a target to learn about neutrons, however, is that the kinematics are “altered”, when it is bound inside a nucleus, by Fermi motion and other nuclear effects. While the complexity of the baryon spectrum is simplified by using a specific meson photoproduction that can tag specific resonances as it turned out with the photoproduction of η -meson off the nucleons. The η works as an isospin filter, due to isospin conservation: only N^* resonances contribute to $N\eta$ while resonances in $\Delta\eta$ belong to the Δ^* series.

The η -meson photoproduction off the proton was widely studied [10, 11, 12, 13, 14, 15, 16, 17, 18, 19, 20]. It was found that the resonance $S_{11}(1535)$ is completely dominating the photoproduction of η -meson at threshold and shows up as bump in the total cross section. Above 1600 MeV in mass location the situation is less clear. The eta-MAID model [21] considers for example the contribution of the resonance $P_{11}(1710)$ while the Bonn-Gatchina model [17, 20, 22] considers the resonance $P_{13}(1730)$. Although the preliminary results of the CB-ELSA/TAPS Collaboration for the double polarization observable E seems to indicate contribution of partial waves with spin 1/2 (for more details see the contribution of R. Beck to this conference proceedings). In general, it is considered that the background terms are pretty low and that the photoproduction of η -mesons involves less than 12 resonances below 2.5 GeV (in invariant mass).

On the other hand the η -meson photoproduction off the neutron is less studied (for the reasons mentioned above) but since a few years it received more attention because four different experiments GRAAL in Grenoble [23], LNS in Sendai [24], CB-ELSA/TAPS in Bonn [9] and more recently A2 in Mainz [25] show a bump structure in the total cross section around 1700 MeV which is not seen in the total cross section of the η -meson photoproduction off the proton. This structure seems to get narrower if the Fermi motion is removed. In absence of double polarization observables, there are no explanations of this so-called “neutron-anomaly”. Nevertheless there are several scenarios proposed. The eta-MAID model [21] attributes this bump to the resonance $D_{15}(1675)$ but the $N\eta$ branching ratio of this state is 17 % in this model. This value is contradictory with other results which give an upper limit of $< 1\%$ [26]. An analysis done with the Bonn-Gatchina model [27] can reproduce the neutron data by taking into account the Fermi motion effect with three completely different scenarios, by either adding a ‘conventionally’ broad P_{11} resonance, a very narrow P_{11} state, or even by adjusting the interference pattern for the S -wave amplitudes. The Giessen coupled channel model [28] can also produce a bump in the neutron excitation around 1 GeV (in photon energy) due to the $S_{11} - P_{11}$ sector, without introducing any additional resonance. Döring and Nakayama [29] can create a bump by using an S -wave coupled channel model in the neutron total cross section which is related to the opening of strangeness thresholds of $K\Lambda$ and $K\Sigma$ photoproduction around 900 MeV and 1050 MeV (for details see the proceeding of M. Döring in which these results were presented). Finally, the chiral soliton model [30, 31] predicted a state in this energy range, which has a much stronger photon coupling to the neutron than to the proton and a large decay branching ratio into $N\eta$. This state is the nucleon-like member of the anti-decuplet of pentaquarks, which would be a P_{11} state but the evidence for the existence of the Θ^+ -pentaquark is strongly doubted.

The results reported here correspond to a new analysis of the data already published [9] where the Fermi motion was removed by reconstructing the η -neutron pairs invariant mass (for all $\cos(\Theta_{\eta}^{cm})$ unlike [9] where it was done for $\cos(\Theta_{\eta}^{cm}) < -0.1$). In addition very preliminary analysis of the A2 Collaboration will be discussed. But first the experimental setups and then the reaction identification of $\gamma + d \rightarrow \eta + n_{participant} + p_{spectator}$ will be shortly described.

CRYSTAL BARREL AND TAPS AT ELSA SETUP

The Bonn real photon beam was made by directing the electron beam (with can reach the maximum energy of 3.5 GeV) on a copper foil, where it produces photons by the Bremsstrahlung process. The photon energies were tagged via the momentum analysis of the scattered electron by a magnetic spectrometer. The Bremsstrahlung photons are nearly collinear with the incident electron beam and pass through a hole in the magnet yoke, after which they are collimated, and then impinge on the deuterium target (of 5.275 cm length) which sits in the center of an almost 4π detection system. It was composed of: the Crystal Barrel (CB, 1290 CsI crystals covering the full azimuthal angle for polar angles between 30° and 168° and the TAPS detectors (528 BaF2 crystals mounted as a hexagonal forward wall covering polar angles down to 4.5°), and their respective Charge Particle Counters (CPC), the inner detector (three

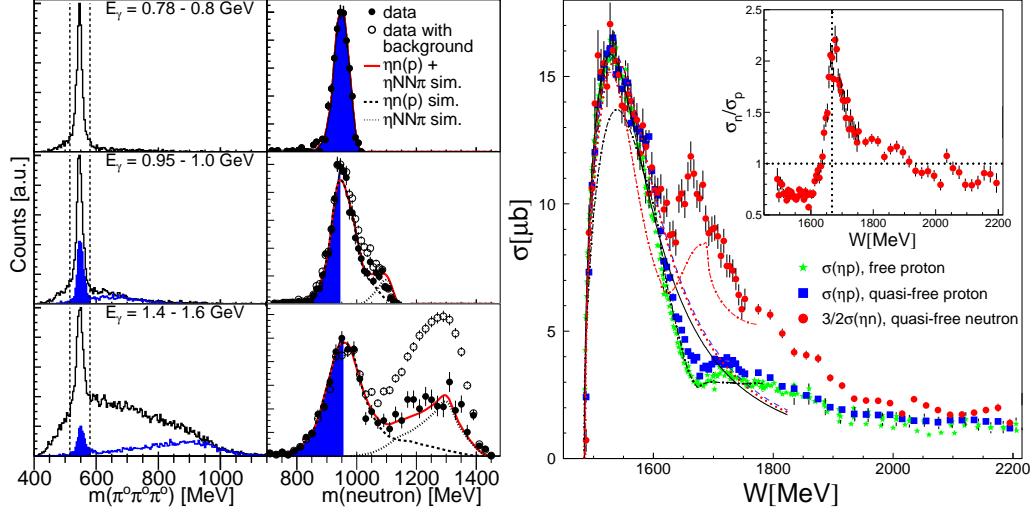


FIGURE 1. Left: Invariant (left hand column) and missing mass (right hand column) spectra for η -mesons in coincidence with recoil neutrons for three ranges of incident photon energy. Invariant masses: shaded (blue) signal after missing mass cut. Dashed lines: applied invariant mass cut. Missing mass data: open symbols represents data for indicated cut on invariant mass. Black dots: background subtracted by fitting invariant mass spectra for each bin of missing mass. Simulations: dashed curves (dotted) curves: simulation of η ($\eta\pi$) final states. Solid (red) curves: sum of simulations. Shaded (blue) areas: accepted events. Right: Total cross sections as function of final state invariant mass W without cut on spectator momentum. (Red) dots: quasi-free neutron, (blue) squares: quasi-free proton, (green) stars: free proton data. Curves: fitted (up to $W = 1600$ MeV) $S_{11}(1535)$ line shapes. (Black) solid: free proton, (blue) dashed: quasi-free proton, (red) dotted: quasi-free neutron. Insert: ratio of quasi-free neutron - proton data. Dash-dotted curves: model results from [29].

layers of plastic scintillating fibers) and the veto wall (528 plastic scintillators). More details can be found in [32].

CRYSTAL BALL AND TAPS AT MAMI SETUP

The Mainz real photon beam was produced in a similar way with a maximum electron energy of 1508 MeV but the beam intensity was an order of magnitude higher than in Bonn. The MAMI-Glasgow tagging spectrometer [33] was used to detect the electrons deflected by a magnetic field. The photon was incident on a 4.6 cm liquid deuterium target or a 5.3 cm liquid helium 3 target installed in the center of the Crystal Ball (CB) [34] made of 672 NaI(Tl) triangular-pyramidal crystals arranged in the form of two hemispheres that has two 21° openings. The downstream opening was covered by the TAPS [35, 36] wall, which consists of 360 BaF₂ crystals, up to 1° . Both detectors had their Charge Particle Identifier (CPI), the particle identification detector (PID) and the veto wall (320 plastic scintillators).

REACTION IDENTIFICATION

Only the reaction identification of $\gamma + d \rightarrow \eta + n_{participant} + p_{spectator}$ (with η decaying into $3\pi^0$) for the CB-ELSA/TAPS experiments will be discussed. We consider all events with seven neutral hits and no charged hits i.e. the CPC did not record a hit. The best combination of $3\pi^0$ is built by using a χ^2 -test on the π^0 mass. The left over hit is considered as a neutron candidate. To check if the $3\pi^0$ and the neutron indeed are the η -neutron pair a missing mass analysis is performed where the detected neutron candidate is treated as a missing neutron and the neutron target is assuming to be at rest: $m(neutron) = \sqrt{(E_\gamma + m_{neutron} - E_\eta)^2 - (\vec{p}_\gamma - \vec{p}_\eta)^2}$. Figure 1 illustrates the missing mass analysis. In the left hand column of the left figure 1, invariant mass spectra of the $3\pi^0$ triplets are plotted for different incident photon energies. The η -resonance is clearly seen. A cut around the η -resonance is done (illustrated by the vertical dashed lines) and the corresponding missing neutron mass spectrum is plotted in the right hand column of the left figure on the left for the same incident photon beam. A peak at the neutron mass is present as expected. With increasing photon beam energy a tale on the missing neutron spectra start to appear. It corresponds to competitive

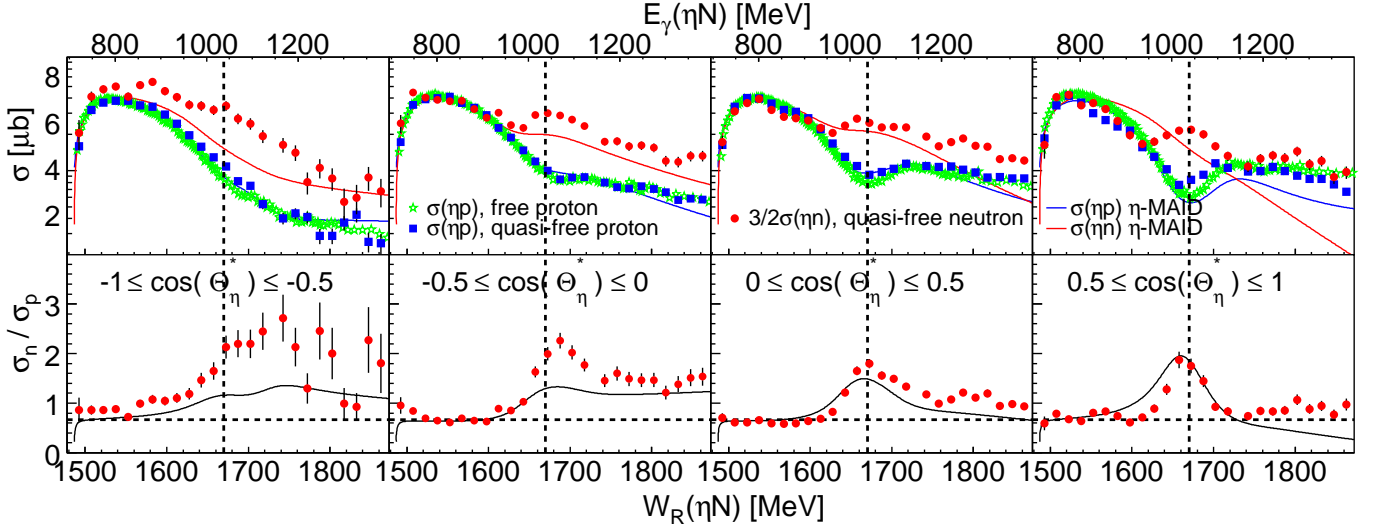


FIGURE 2. First row: excitation functions for different bins of η cm polar angle. (Blue) open squares: quasi-free proton data, (black) stars: free proton data from [40] (also presented at this conference by Igor Strakovsky), (red) dots: quasi-free neutron data scaled up by 3/2. (Blue) solid lines: η -MAID [21] for proton, (red) dashed lines: η -MAID for neutron. Second row: ratio of neutron and proton cross section for data and η -MAID.

background channels - $\eta\pi$ -, where the pion (either charged or neutral) was not detected. The line shape of the missing neutron mass spectrum was reproduced by a GEANT-based Monte Carlo simulation [37] to model the response of the detector by taking into account the signal and the background channels. A conservative cut was chosen represented by the blue area on the right hand figure. The $3\pi^0$ signal remaining after the cut on the missing neutron spectra are also in blue (left hand figure). The remaining combinatorial background below the η -resonance was removed by a fit estimating the η signal.

RESULTS

A summary of the results is plotted in Figure 1 (right). The η -nucleon pairs are reconstructed using the fact that the reaction kinematics is exactly determined. The nucleon energy is calculated by the relation linking the following measured or reconstructed quantities: the η four vector, the incident photon beam energy and the nucleon angles. Details about the efficiency corrections and the absolute normalization are discussed in [38, 39]. The η -proton pairs invariant mass spectrum $\sigma(\eta p)$ (blue square) and the free proton data (green star) are in good agreement showing that the Fermi motion can be effectively removed and that the other nuclear effects are negligible. Furthermore a preliminary analysis of the liquid ${}^3\text{He}$ data taken by the A2 Collaboration [41] also shows a bump like structure which is ruling out any nucleus effect. The η -neutron pairs invariant mass spectrum $\sigma(\eta n)$ (red point) is scaled by a factor of 3/2. $\sigma(\eta n)$ and $\sigma(\eta p)$ have the same shape as expected in the $S_{11}(1535)$ energy region. Around 1.7 GeV a narrow structure is clearly seen in $\sigma(\eta n)$ and is absent from $\sigma(\eta p)$.

However, the excitation functions for different bins of η cm polar angle, see Figure 2, highlight an intriguing opposite behavior between $\sigma(\eta n)$ and $\sigma(\eta p)$. A bump-like structure is visible for all bins of η cm polar angle at ≈ 1670 MeV which is changing for the different bins, while no bump-like structure is seen for the proton but a dip starts to appear for forward η cm polar angles. At very forward angles the bump and the dip are symmetric. This behavior finally creates the bump - dip structures of the total cross sections. A possible interpretation is that two different processes occurs: an interference between amplitudes belonging to different partial waves (excitation functions - Figure 2) and a single amplitude or an interference between amplitudes belonging to the same partial waves (total cross section - Figure 1). Finally the η -neutron pairs invariant mass spectrum was fitted: in the $S_{11}(1535)$ energy region a parameterization of a Breit-Wigner curve with energy dependent width [42] and two further simple Breit-Wigner curves with constant width ($x \equiv 1$). The results of fit give $W \approx 1665$ MeV and with a FWHM $\Gamma = 25$ MeV.

CONCLUSION

The Fermi motion can be effectively removed as shown by the good agreement between the free proton data and the quasi-free proton data. A narrow structure at $W \approx 1665$ MeV and with a FWHM of $\Gamma = 25$ MeV is seen in the invariant mass spectrum of the η -neutron pairs which is not due to a nucleus effect. This structure is not seen in the invariant mass spectrum of the η -proton pairs but an opposite behavior is seen in the excitation functions for different bins of η cm polar angle.

ACKNOWLEDGMENTS

We wish to acknowledge the outstanding support of the accelerator groups and operators of ELSA and of MAMI. This work was supported by Schweizerischer Nationalfonds and Deutsche Forschungsgemeinschaft (SFB/TR-16).

REFERENCES

1. D. E. Groom et al., *Eur. Phys. J. C* **15**, 1 (2000).
2. M. Kirchbach, *Mod. Phys. Lett. A* **12**, 3177 (1997).
3. B. Mecking et al., *Nucl. Instr. and Meth.* **94**, 262 (2003).
4. D. Husman, W.J. Schwille, *Phys. BL* **44**, 40 (1988).
5. W. Hillert, *Eur. Phys. J. A* **28**, 139 (2006).
6. H. Herminghaus et al., *IEEE Trans. Nucl. Sci.* **30**, 3274 (1983).
7. K.-H. Kaiser et al., *Nucl. Instrum. Methods A* **593**, 159 (2008).
8. Moorhouse, *Phys. Rev. Lett.* **16**, 771 (1966)
9. Jaegle et al., *Phys. Rev. Lett.* **100**, 252002 (2008).
10. B. Krusche et al., *Phys. Rev. Lett.* **74**, 3736 (1995).
11. J. Ajaka et al., *Phys. Rev. Lett.* **81**, 1797 (1998).
12. A. Bock et al., *Phys. Rev. Lett.* **81**, 534 (1998).
13. C.S. Armstrong et al., *Phys. Rev. D* **60**, 052004 (1999).
14. R. Thompson et al., *Phys. Rev. Lett.* **86**, 1702 (2001).
15. F. Renard et al., *Phys. Lett. B* **528**, 215 (2002).
16. M. Dugger et al., *Phys. Rev. Lett.* **89**, 222002 (2002).
17. V. Crede et al., *Phys. Rev. Lett.* **94**, 012004 (2005).
18. T. Nakabayashi et al., *Phys. Rev. C* **74**, 035202 (2006).
19. O. Bartholomy et al., *Eur. Phys. J. A* **33**, 133 (2007).
20. D. Elsner et al., *Eur. Phys. J. A* **33**, 147 (2007).
21. W.-T. Chiang et al., *Nucl. Phys. A* **700**, 429 (2002).
22. V.A. Anisovich et al., *Eur. Phys. J. A* **25**, 427 (2005).
23. V. Kuznetsov et al., *Phys. Lett. B* **647**, 23 (2007).
24. F. Miyahara et al., *Prog. Theor. Phys. Suppl.* **168**, 90 (2007).
25. D. Werthmüller for the Crystal Ball/TAPS collaborations, *Chinese Physics C* **33** (12): 1345-1348 (2009)
26. K. Nakamura et al., *Journal of Physics G* **37**, 075021 (2010).
27. V.A. Anisovich et al., *Eur. Phys. J. A* **41**, 13 (2009).
28. V. Shklyar, H. Lenske, U. Mosel, *Phys. Lett. B* **650**, 172 (2007).
29. M. Döring and K. Nakayama, *Phys. Lett. B* **683**, 145 (2010).
30. M. Polyakov and A. Rathke, *Eur. Phys. J. A* **18**, 691 (2003).
31. R.A. Arndt et al., *Phys. Rev. C* **69**, 035208 (2004).
32. T. Mertens et al., *Eur. Phys. J. A* **38**, 195 (2008).
33. I. Anthony et al., *Nucl. Instr. Meth. A* **301**, 230 (1991).
34. M. Oreglia et al., *Phys. Rev. D* **25**, 2259 (1982).
35. R. Novotny, *IEEE Trans. on Nucl. Science* **38**, 379 (1991).
36. A.R. Gabler et al., *Nucl. Instr. and Meth. A* **346**, 168 (1994).
37. R. Brun et al., GEANT 3.21, CERN DD/EE/84-1, 1984
38. Jaegle et al., *Eur. Phys. J. A* **47**, 11 (2011).
39. Jaegle et al., Quasi-free photoproduction of η -mesons off the deuteron to be submitted in EPJA.
40. E.F. McNicoll et al., *Phys. Rev. C* **82**, 035208 (2010).
41. L. Witthauer et al., under preparation,
42. B. Krusche and S. Schadmand, *Prog. Part. Nucl. Phys.* **51**, 399 (2003).